# Switch-Mode Continuously Variable Transmission: Modeling and Optimization

**James D. Van de Ven**
e-mail: vandeven@wpi.edu

**Michael A. Demetriou**
e-mail: mdemetri@wpi.edu

Department of Mechanical Engineering,
Worcester Polytechnic Institute,
100 Institute Road,
Worcester, MA 01609

*Hybrid vehicles are an important step toward reducing global petroleum consumption and greenhouse gas emissions. Flywheel energy storage in a hybrid vehicle combines high energy density and high power density, yet requires a highly efficient continuously variable transmission with a wide operating range. This paper presents a novel solution to coupling a high-speed flywheel to the drive train of a vehicle, the switch-mode continuously variable transmission (CVT). The switch-mode CVT, the mechanical analog of a boost converter from power electronics, utilizes a rapidly switching clutch to transmit energy from a flywheel to a spring, which applies a torque to the drive train. By varying the duty ratio of the clutch, the average output torque is controlled. This paper examines the feasibility of this concept by formulating a mathematical model of the switch-mode CVT, which is then placed in state-space form. The state-space formulation is leveraged to analyze the system stability and perform simple optimization of the switch time and damping rate of the spring over the first switching period. The results of this work are that a stable equilibrium does exist when the speed of the output shaft is zero, but the system will not reach and stay at a desired torque if this condition is not met, but requires continuous switching between the two states. An optimal switching time and damping ratio were found for the given parameters, where the lowest error occurred with low values of damping ratio. This work builds a foundation for future work in increasing the complexity of the model and the optimization method.* [DOI: 10.1115/1.4003373]

## 1 Introduction

Currently, petroleum combustion is a prime source of global energy, with the largest consumption in the transportation industry. In 2008, the transportation industry in the United States consumed $5\times10^9$ barrels of petroleum, $2.8\times10^9$ barrels of which were consumed by passenger cars [1]. The social, economic, and environmental issues related to the consumption of fossil fuels elevate the importance of improving vehicle efficiency. Through regenerative braking, eliminating idling losses, and aggressive engine management, hybrid vehicle drive trains create significant improvements in vehicle efficiency [2].

Numerous energy storage mediums have been proposed for hybrid vehicles including batteries, capacitors, hydraulic accumulators, flywheels, elastomeric springs, and others. Of these technologies, two technologies are emerging in the market: electric hybrids with battery energy storage and hydraulic hybrids with hydraulic accumulator energy storage. Electric systems provide a high energy density storage, at 220–540 kJ/kg for nickel-metal hydride and lithium ion batteries, respectively [3], yet suffer from limited power density of approximately 30–100 W/kg [4]. Hydraulic system provides very high power density of approximately 500–1000 W/kg [4], yet is limited in energy density to approximately 5 kJ/kg for modern composite accumulators [2].

Utilizing a flywheel for auxiliary energy storage in a hybrid vehicle combines high energy density at approximately 325 kJ/kg [5] with extremely high power density that is only limited by the torque capabilities of the mechanical components [6]. The prime challenge facing flywheel energy storage is the need for an efficient transmission to couple the high-speed flywheel with the wheels of the vehicle. Previous work in this field has proposed continuously variable transmissions (CVTs) using hydraulics, belt drives, and toroidal drives, with marginal success [7,8]. Another approach involves an electric generator-motor transmission, yet this creates the same power density limitations of an electric system [9]. Recent work is emerging in the area of flywheel energy storage for Formula (1) race cars, utilizing a toroidal CVT [10].

This paper presents a novel transmission for a flywheel hybrid drive train: the switch-mode continuously variable transmission, which is the mechanical analog of a dc-dc switch-mode converter from the field of power electronics [11]. The switch-mode CVT operates in distinct on and off modes, using a high frequency pulsing clutch to transmit energy from a flywheel to a spring connected to the drive train. A similar concept that utilized two clutches and a spring connected to ground was previously described and tested by Gilbert et al. This previous work transmitted low levels of power through limited ranges of 1:3.2 and 1.3:1 [12]. The design did not enable energy storage and relied on oscillating the spring connected to ground for operation.

Based on the aforementioned need for alternative energy storage, this manuscript examines the feasibility of the switch-mode continuously variable transmission. A mathematical model capturing the salient features of the switch-mode CVT is presented in Sec. 3 after a brief description of such a transmission in Sec. 2. Such a mathematical model will serve to understand the dynamics of the switch-mode CVT and subsequently improve and optimize its design before a prototype is built. The resulting equations of motion are then placed in state-space form in order to take advantage of already existing results on stability analysis of switched systems and parameter optimization. A detailed account of this state-space formulation is presented in Sec. 4. In this first effort on optimization of switch-mode CVT, a simple (brute force) optimization is performed over a single duty cycle and summarized also in Sec. 4. Such a preliminary optimization study provides substantial insight on the behavior of the switch-mode CVT and forms the foundation for a more involved optimization of a detailed mathematical model. Numerical results on the simple optimization are presented in Sec. 5 and conclusions along with future research follow in Sec. 6.

Contributed by the Dynamic Systems Division of ASME for publication in the JOURNAL OF DYNAMIC SYSTEMS MEASUREMENT, AND CONTROL. Manuscript received December 15, 2009; final manuscript received August 10, 2010; published online March 24, 2011. Assoc. Editor: Luis Alvarez.

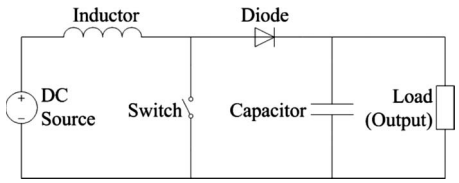


**Fig. 1 A boost power converter increases the voltage from the input source to the output by controlling the duty cycle of the switch**

## 2 Description of Switch-Mode CVT

The switch-mode CVT presented in this paper is the mechanical analog of a step-up (boost) converter from power electronics. The electrical circuit, shown in Fig. 1, uses two energy storage devices, an inductor and a capacitor, along with an on-off switch and a diode to produce an output voltage that is larger than the input voltage [11]. The average output voltage is controlled by varying the duty cycle, defined as the time the switch is in the on position divided by the switching period.

The switch-mode CVT is formulated by replacing the electrical components of the boost converter circuit with mechanical components. The inductor is replaced with a flywheel, the capacitor by a spring, the switch by a clutch, and the diode by an antireversing ratchet or one-way locking bearing. This formulation, shown in Fig. 2, varies the output torque by controlling the duty ratio of the clutch. This architecture also enables the drive train to store a significant quantity of energy in the flywheel.

The operation of the switch-mode CVT contains two distinct states. In the *on-state*, the clutch is engaged causing the input side of the spring and the flywheel rotate at the same angular velocity, increasing the deflection of the spring and thus the torque applied to the output shaft. In the *off-state*, the clutch is disengaged and torque applied to the input shaft increases the angular velocity of the flywheel. During this mode, the ratchet prevents backward rotation of the input side of the rotational spring, while the spring applies a torque to the output shaft. Modulating the duty cycle of the clutch controls the output torque. It does need to be noted that the switch-mode CVT does not vary through specific gear ratios as in a conventional transmission. Instead, the output torque is controlled by the duty ratio of the clutch.

For the switch-mode CVT to operate in a hybrid vehicle, during regenerative events, such as braking or descending a grade, a method of storing energy in the flywheel is required. In the CVT architecture described above, the torque reversal created during regeneration results in freewheeling of the ratchet and no energy storage. To allow regeneration, two components are added to the system: a brake on the intermediate shaft and an over-running clutch between the intermediate shaft and the flywheel, as seen in Fig. 3. During regeneration, the brake is engaged and the spring deflects, applying a negative torque to the output shaft. The stored energy in the spring is transferred to the flywheel by disengaging the brake, causing the over-running clutch to engage. Once the deflection in the spring returns to zero, the over-running clutch

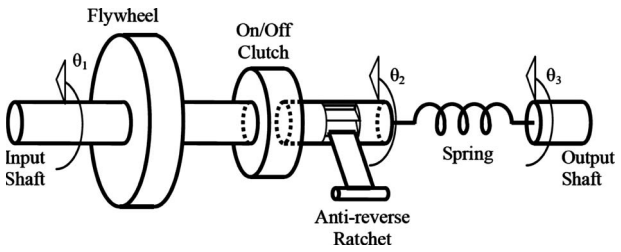


**Fig. 2 The switch-mode CVT controls the torque transmitted to the output shaft by specifying the duty cycle of the clutch**

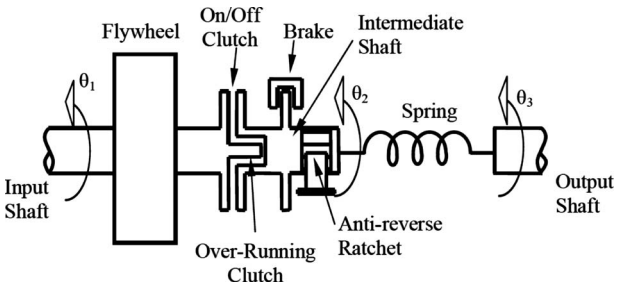


**Fig. 3 The switch-mode CVT with the additional components required for regenerative operation. In regenerative operation, the brake is pulsed to create deflection in the spring and the over-running clutch transmits torque to the flywheel.**

operates in freewheel mode. Rapidly switching the brake on and off with a controlled duty ratio modulates the regenerative torque similar to controlling the clutch for generative mode. The additions of the brake and over-running clutch do not influence the generative operation.

## 3 Dynamic System Equations

To model the switch-mode CVT, dynamic system equations are required for both the on- and off-states in generative and regenerative operations. To aid in developing the equations of motion, free-body-diagrams are created of the individual components, as shown in Fig. 4. This analysis makes several assumptions including the following: The inertia of the flywheel and the clutch are combined and represented by $I_1$, the inertia of the output shaft and the vehicle kinetic energy are combined into a second flywheel with inertia $I_3$, the output of the clutch (intermediate shaft) is assumed to have negligible inertia, the rotational spring is modeled as a perfect spring and a rotational damper, and the engagement and disengagement of the clutch are instantaneous.

In the generative mode, when the clutch is engaged, the system is in the on-state. During this state, the system can be represented by the following dynamic equations:

$$I_1\ddot{\theta}_1 + b(\dot{\theta}_2 - \dot{\theta}_3) + k(\theta_2 - \theta_3) = T_{\text{in}}(t) \tag{1}$$

$$I_3\ddot{\theta}_3 - b(\dot{\theta}_2 - \dot{\theta}_3) - k(\theta_2 - \theta_3) = -T_{\text{out}}(t) \tag{2}$$

$$\dot{\theta}_2 = \dot{\theta}_1 \tag{3}$$

where $\theta_1$, $\theta_2$, and $\theta_3$ are the angular positions of the input shaft, input side of the spring, and the output shaft, respectively, $b$ is the damping rate of the spring, $k$ is the spring rate, and $T_{\text{in}}(t)$ and $T_{\text{out}}(t)$ are the input and output torques, respectively. The angular velocity and angular acceleration are expressed by $\dot{\theta}$ and $\ddot{\theta}$, respectively.

When the clutch is disengaged in the generative mode, the system is in the off-state. During this state, the spring is disengaged from the flywheel and the left side of the spring is held stationary by the ratchet. In this state, the dynamic system equations simplify to

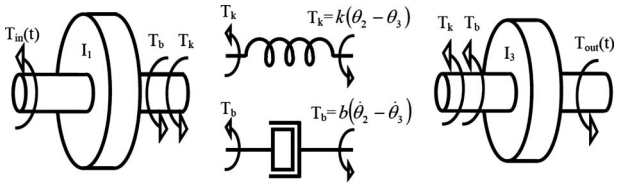


**Fig. 4 Simplified free-body-diagrams of the components of the switch-mode CVT**

**Table 1 System parameters used in the analysis**

| Parameter | Symbol | Value | Units |
|---|---|---|---|
| Input flywheel inertia | $I_1$ | 0.328 | kg m$^2$ |
| Output flywheel inertia | $I_3$ | 210.9 | kg m$^2$ |
| Spring rate | $k$ | 995 | N m/rad |
| Spring damping rate | $b$ | 55.0 | N m s/rad |
| Initial angular velocity of input flywheel | $\dot{\theta}_1(t_o)$ | 2100 | rad/s |
| Initial angular velocity of output flywheel | $\dot{\theta}_3(t_o)$ | 0 | rad/s |
| Switching frequency | $f$ | 20 | Hz |

$$I_1\ddot{\theta}_1 = T_{\text{in}}(t) \tag{4}$$

$$I_3\ddot{\theta}_3 - b(\dot{\theta}_2 - \dot{\theta}_3) - k(\theta_2 - \theta_3) = -T_{\text{out}}(t) \tag{5}$$

$$\dot{\theta}_2 = 0 \tag{6}$$

In the case that the stored energy in the spring is zero, which occurs when $\theta_2 - \theta_3 \leq 0$, the ratchet allows the input side of the spring $\theta_2$ to freely rotate. For this case, Eq. (6) is replaced with

$$\dot{\theta}_2 = \dot{\theta}_3 \tag{7}$$

During regeneration, the on-state occurs when the brake on the intermediate shaft is engaged. During this state, the over-running clutch between the flywheel and the intermediate shaft is freewheeling and the deflection in the spring is increasing and creating a negative torque on the output shaft due to holding the intermediate shaft stationary with the brake. During this state, the system can be described by

$$I_1\ddot{\theta}_1 = T_{\text{in}}(t) \tag{8}$$

$$I_3\ddot{\theta}_3 - b(\dot{\theta}_2 - \dot{\theta}_3) - k(\theta_2 - \theta_3) = -T_{\text{out}}(t) \tag{9}$$

$$\dot{\theta}_2 = 0 \tag{10}$$

When the brake is released during regeneration, the system is in the off-state. In the regenerative off-state, the over-running clutch engages due to the negative torque in the intermediate shaft and energy is transferred from the spring to the flywheel. In this state, the system is described by

$$I_1\ddot{\theta}_1 + b(\dot{\theta}_2 - \dot{\theta}_3) + k(\theta_2 - \theta_3) = T_{\text{in}}(t) \tag{11}$$

$$I_3\ddot{\theta}_3 - b(\dot{\theta}_2 - \dot{\theta}_3) - k(\theta_2 - \theta_3) = -T_{\text{out}}(t) \tag{12}$$

$$\dot{\theta}_2 = \dot{\theta}_1 \tag{13}$$

Once the stored energy in the spring is zero in the regenerative off-state, which occurs when $\theta_2 - \theta_3 \geq 0$, the over-running clutch disengages and Eq. (13) is replaced with

$$\dot{\theta}_2 = \dot{\theta}_3 \tag{14}$$

**3.1 System Parameters.** To provide physical meaning to the analysis that follows, Table 1 presents a list of system parameters and initial conditions that represent implementation of the switch-mode CVT into the drive train of a 1500 kg passenger vehicle. The input flywheel inertia and initial angular velocity represent storing sufficient energy to accelerate the vehicle to 31.3 m/s (70 mph), assuming a flywheel angular velocity of 2100 rad/s. It should be noted that this angular velocity likely requires the flywheel to be mounted in a vacuum chamber with magnetic bearings. The output flywheel inertia is size to convert the linear momentum of the vehicle into the equivalent angular momentum, assuming a 0.75 m diameter tire. The spring rate was selected based on a desired maximum torque of 12,500 N m at a deflection of two full rotations of the spring. Finally, the damping rate of the spring was selected by assuming a damping ratio of 0.06, which is typical for mechanical systems [13]. The influence of the damping ratio will be further explored in the optimization below.

## 4 State-Space Formulation

To analyze the above set of equations for both the on-state and off-state, we express them in state-space form, which is conducive to both stability analysis and optimization. Optimization will be performed on the percentage of the duty cycle that the on-state is active and subsequently on the optimal values of the rotational spring parameters, such as the damping ratio. Toward this end, we define the following state variables:

$$x(t) = \begin{bmatrix} x_1(t) \\ x_2(t) \\ x_3(t) \\ x_4(t) \\ x_5(t) \end{bmatrix} = \begin{bmatrix} \theta_1(t) \\ \theta_3(t) \\ \dot{\theta}_1(t) \\ \dot{\theta}_3(t) \\ \theta_2(t) \end{bmatrix} \tag{15}$$

Equations (1)–(3) describing the on-state during generative operation can now be written as

$$\dot{x}(t) = \begin{bmatrix} \dot{x}_1(t) \\ \dot{x}_2(t) \\ \dot{x}_3(t) \\ \dot{x}_4(t) \\ \dot{x}_5(t) \end{bmatrix} = \begin{bmatrix} \dot{\theta}_1(t) \\ \dot{\theta}_3(t) \\ \ddot{\theta}_1(t) \\ \ddot{\theta}_3(t) \\ \dot{\theta}_2(t) \end{bmatrix} = \begin{bmatrix} x_3(t) \\ x_4(t) \\ -\frac{k}{I_1}x_1(t) + \frac{k}{I_1}x_2(t) - \frac{b}{I_1}x_3(t) + \frac{b}{I_1}x_4(t) + \frac{1}{I_1}T_{\text{in}}(t) \\ \frac{k}{I_3}x_1(t) - \frac{k}{I_3}x_2(t) + \frac{b}{I_3}x_3(t) - \frac{b}{I_3}x_4(t) - \frac{b}{I_3}T_{\text{out}}(t) \\ x_3(t) \end{bmatrix} \tag{16}$$

or in state-space form

$$\dot{x}(t) = \begin{bmatrix} 0 & 0 & 1 & 0 & 0 \\ 0 & 0 & 0 & 1 & 0 \\ -\frac{k}{I_1} & \frac{k}{I_1} & -\frac{b}{I_1} & \frac{b}{I_1} & 0 \\ \frac{k}{I_3} & -\frac{k}{I_3} & \frac{b}{I_3} & -\frac{b}{I_3} & 0 \\ 0 & 0 & 1 & 0 & 0 \end{bmatrix} \begin{bmatrix} x_1(t) \\ x_2(t) \\ x_3(t) \\ x_4(t) \\ x_5(t) \end{bmatrix} + \begin{bmatrix} 0 \\ 0 \\ \frac{1}{I_1} \\ 0 \\ 0 \end{bmatrix} T_{\text{in}}(t) + \begin{bmatrix} 0 \\ 0 \\ 0 \\ -\frac{1}{I_3} \\ 0 \end{bmatrix} T_{\text{out}}(t) = A_{\text{on}}x(t) + B_{\text{in}}T_{\text{in}}(t) + B_{\text{out}}T_{\text{out}}(t), \tag{17}$$

$$t \in [(i-1)\Delta t, t_s^i]$$

where $\Delta t$ denotes the duration of a duty cycle and $t_s^i$ denotes the switch time from the on-state to the off-state during the $i$th duty

cycle. Similarly, for the off-state, Eqs. (4)–(6) become

$$\dot{x}(t) = \begin{bmatrix} 0 & 0 & 1 & 0 & 0 \\ 0 & 0 & 0 & 1 & 0 \\ 0 & 0 & 0 & 0 & 0 \\ 0 & -\frac{k}{I_3} & 0 & -\frac{b}{I_3} & \frac{k}{I_3} \\ 0 & 0 & 0 & 0 & 0 \end{bmatrix} \begin{bmatrix} \dot{x}_1(t) \\ \dot{x}_2(t) \\ \dot{x}_3(t) \\ \dot{x}_4(t) \\ \dot{x}_5(t) \end{bmatrix} + \begin{bmatrix} 0 \\ 0 \\ \frac{1}{I_1} \\ 0 \\ 0 \end{bmatrix} T_{\text{in}}(t) + \begin{bmatrix} 0 \\ 0 \\ 0 \\ -\frac{1}{I_3} \\ 0 \end{bmatrix} T_{\text{out}}(t) = A_{\text{off}}x(t) + B_{\text{in}}T_{\text{in}}(t) + B_{\text{out}}T_{\text{out}}(t),$$

$$t \in (t_s^i, i\Delta t] \tag{18}$$

The dynamics of the switch-mode CVT over a given duty cycle are compactly given by the following switched dynamical system:

$$\dot{x}(t) = \begin{cases} A_{\text{on}}x(t) + B_{\text{in}}T_{\text{in}}(t) + B_{\text{out}}T_{\text{out}}(t), & t \in [(i-1)\Delta t, t_s^i] \\ A_{\text{off}}x(t) + B_{\text{in}}T_{\text{in}}(t) + B_{\text{out}}T_{\text{out}}(t), & t \in (t_s^i, i\Delta t] \end{cases} \tag{19}$$

The *goal* is to make the torque due to the rotational spring $k(\theta_2(t) - \theta_3(t))$ match the output torque $T_{\text{out}}(t)$ by controlling the switch time $t_s^i$ over a given duty cycle. In state-space form, the rotational spring torque is viewed as the observed output signal and in this case it is given by

$$y(t) = k(\theta_2(t) - \theta_3(t)) = \begin{bmatrix} 0 & -k & 0 & 0 & k \end{bmatrix} \begin{bmatrix} x_1(t) \\ x_2(t) \\ x_3(t) \\ x_4(t) \\ x_5(t) \end{bmatrix} = Cx(t) \tag{20}$$

The control objective can now be expressed in terms of the state-space formulation of the on-state and off-state equations so that the output $y(t)$ equals the output torque.

As it will be elaborated in the stability analysis below, the output $y(t)$ will never *reach and stay* at the output torque $T_{\text{out}}(t)$ when the CVT is switched between the on-state and the off-state. Therefore, one would like to minimize the deviation of the output $y(t)$ from the output torque. An appropriate metric for this deviation is the $L_2$ norm of the difference $y(t) - T_{\text{out}}(t)$. The evolution of the output $y(t)$ in a typical run over a 10 cycle duration is depicted in Fig. 5, where it is observed that the largest contribution to the $L_2$ error norm occurs during the first cycle. The way that switching occurred in this simple run was based on the following pseudocode:

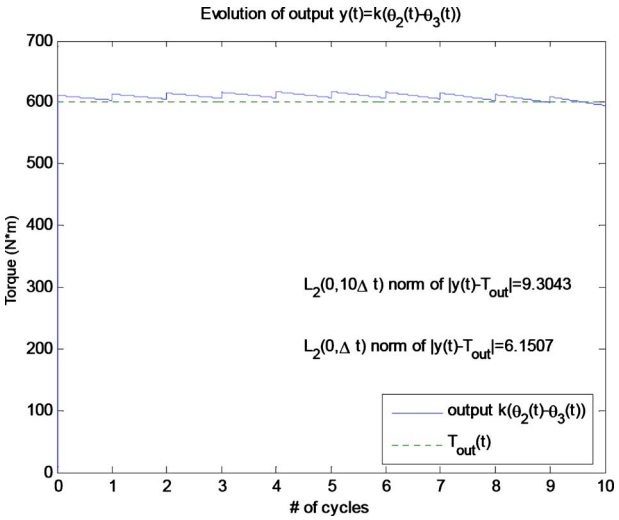


**Fig. 5 Evolution of output $y(t)$ over 10 cycles**

$$\begin{cases} \text{initialize with on-state} \\ \text{if } y(t) - T_{\text{out}} > 0.01T_{\text{out}} \text{ then} \\ \text{switch to off-state} \end{cases} \tag{21}$$

As a first approach in our stability and optimization approach, we consider the evolution of the above system over a single duty cycle and attempt to find the optimal switch time that would enable the output $y(t)$ to track the output torque $T_{\text{out}}(t)$. Thus, the switching decision is based on minimizing the error norm of $y(t) - T_{\text{out}}(t)$.

**4.1 Stability Analysis and Optimization Over a Single Duty Cycle.** To gain an insight on the switching from the on-state to the off-state, let us consider the dynamics for $\theta_3(t)$ over a single duty cycle while in the off-state, i.e., Eq. (5),

$$\begin{cases} I_3\ddot{\theta}_3(t) + b(\dot{\theta}_3(t) - \dot{\theta}_2(t)) + k(\theta_3(t) - \theta_2(t)) = -T_{\text{out}}(t), & t \in (t_s, \Delta t] \\ \theta_3(t_s) = \theta_3(t_s^-), & \dot{\theta}_3(t_s) = \dot{\theta}_3(t_s^-) \end{cases} \tag{22}$$

In the off-state, we also have from Eq. (6)

$$\dot{\theta}_2(t) = 0 \tag{23}$$

and therefore

$$\theta_2(t) = \theta_2(t_s^-) = \text{const}, \quad t \in (t_s, \Delta t] \tag{24}$$

where $\theta_2(t_s^-)$ denotes the final value of $\theta_2(t)$ during the on-state, which becomes the initial condition during the off-state. Assuming that the output torque $T_{\text{out}}$ is constant over a given cycle and that the input torque is zero, then this changes the $\theta_3(t)$ dynamics to

$$\begin{cases} \ddot{\theta}_3(t) + \frac{b}{I_3}\dot{\theta}_3(t) + \frac{k}{I_3}\theta_3(t) = \frac{k}{I_3}\theta_2(t_s^-) - \frac{1}{I_3}T_{\text{out}}, & t \in (t_s, \Delta t] \\ \theta_3(t_s) = \theta_3(t_s^-), & \dot{\theta}_3(t_s) = \dot{\theta}_3(t_s^-) \end{cases} \tag{25}$$

This dynamical system has an equilibrium point

$$(\bar{\theta}_3, \dot{\bar{\theta}}_3) = (\theta_2(t_s^-) - T_{\text{out}}/k, 0) \tag{26}$$

which is an exponentially stable equilibrium; i.e., all trajectories of the above differential equation exponentially converge to the

equilibrium values [14]; if the initial conditions of the above differential equation are chosen the same as the equilibrium values, the solution to the differential equation remains at the equilibrium values. This is summarized in the following lemma.

*Lemma 1.* Consider the dynamical system describing the $\theta_3(t)$ dynamics during the off-state, as given in Eq. (22). With the assumption of zero input torque and a constant output torque over a given cycle, one has that dynamical systems (22) and (23) have a unique equilibrium point given in Eq. (26), and it is exponentially stable.

*Proof of Lemma 1.* The proof follows from the stability of second order linear systems in Ref. [14]. Due to the assumption of constant output torque and in view of Eq. (23) along with the fact that the physical parameters are positive constants, then equilibrium point (26) is unique and it is exponentially stable. ■

In order to ensure that the output tracks the output torque, we must then find the switch time $t_s$ during the on-state such that

$$\theta_3(t_s) = \theta_2(t_s) - T_{\text{out}}/k \quad \text{and} \quad \dot{\theta}_3(t_s) = 0 \tag{27}$$

At this specific time instance $t_s$, when the system is switched from the on-state to the off-state, the $\theta_3(t)$ dynamics will remain at the equilibrium point given in Eq. (26), namely,

$$\theta_3(t) = \theta_2(t_s^-) - \frac{T_{\text{out}}}{k} \quad \text{and} \quad \dot{\theta}_3(t) = 0, \quad \forall\, t \in (t_s, \Delta t] \tag{28}$$

If both conditions in Eq. (26) are satisfied *simultaneously* at the switch time $t_s$, then the above stability analysis guarantees that they will stay at their equilibrium values, namely, the output $y(t)$ will stay at the constant value of the output torque $T_{\text{out}}$ throughout the duration of the cycle and the derivative of $\theta_3(t)$ will stay at zero. However, it may not be feasible to satisfy both conditions simultaneously. Therefore, one would like to optimize the switched system by finding the switch time $t_s$ from on-state to off-state that would minimize an appropriate measure of the deviation of $y(t)$ from $T_{\text{out}}$. One such measure of deviation is the root-mean-square error

$$\text{error}_{\text{rms}} = \sqrt{\frac{1}{\Delta t}\left(\int_0^{t_s} (y_{\text{on}}(t) - T_{\text{out}})^2 dt + \int_{t_s}^{\Delta t} (y_{\text{off}}(t) - T_{\text{out}})^2 dt\right)} \tag{29}$$

where $y_{\text{on}}(t) \triangleq y(t)$ for $t \in [0, t_s]$ and $y_{\text{off}}(t) \triangleq y(t)$ for $t \in (t_s, \Delta t]$ in Eq. (19). Alternatively, one may minimize the $L_2(0, \Delta t)$ norm of the error given by[1]

$$\|y(t) - T_{\text{out}}\|^2_{L_2(0,\Delta t)} = \left(\int_0^{t_s} (y_{\text{on}}(t) - T_{\text{out}})^2 dt + \int_{t_s}^{\Delta t} (y_{\text{off}}(t) - T_{\text{out}})^2 dt\right) \tag{30}$$

Therefore the optimization problem is to find the switch time that minimizes the error norm over a single duty cycle

[1]The correct notation for the output $y(t)$ should be $y(t;t_s)$ since the output of the switched dynamical system depends on both the time $t$ in $[0, \Delta t]$ and on the switch time instance $t_s$. However, we hope that this seemingly minor abuse of mathematical notation will not cause any confusion.

$$(\text{Optimization I}) \begin{cases} \text{minimize} \ \ \|y(t) - T_{\text{out}}\|^2_{L_2(0,\Delta t)} \\ \text{subject to} \\ \dot{x}(t) = \begin{cases} A_{\text{on}} x(t) + B_{\text{in}} T_{\text{in}}(t) + B_{\text{out}} T_{\text{out}}(t), & t \in [0, t_s] \\ A_{\text{off}} x(t) + B_{\text{in}} T_{\text{in}}(t) + B_{\text{out}} T_{\text{out}}(t), & t \in (t_s, \Delta t] \end{cases} \\ y(t) = Cx(t) \end{cases} \tag{31}$$

The optimal switch time is then written as

$$t_s = \arg \min_{t \in (0,\Delta t)} \left(\int_0^t (y_{\text{on}}(\tau) - T_{\text{out}})^2 d\tau + \int_t^{\Delta t} (y_{\text{off}}(\tau) - T_{\text{out}})^2 d\tau\right). \tag{32}$$

The above optimization provides the optimal switching time $t_s$ from the on-state to the off-state over the first duty cycle resulting in the smallest possible error norm. However, one may be able to design the torsional spring, via the variation of its damping coefficient, so that it would provide the smallest possible error norm. A subsequent level of optimization may then be incorporated that finds the optimal value of the switch time for different values of the damping parameter $b$. Toward that end, it is assumed that the damping parameter lies in a specific range $b_1 < b < b_2$ dictated by design considerations, and therefore the two state matrices $A_{\text{on}}$ and $A_{\text{off}}$ are now parametrized by the values of $b \in [b_1, b_2]$ as follows:

$$\dot{x}(t;b) = \begin{cases} A_{\text{on}}(b) x(t;b) + B_{\text{in}} T_{\text{in}}(t) + B_{\text{out}} T_{\text{out}}(t), & t \in [(i-1)\Delta t, t_s^i] \\ A_{\text{off}}(b) x(t;b) + B_{\text{in}} T_{\text{in}}(t) + B_{\text{out}} T_{\text{out}}(t), & t \in (t_s^i, i\Delta t] \end{cases}, \quad b \in [b_1, b_2]$$

$$y(t;b) = \begin{bmatrix} 0 & -k & 0 & 0 & k \end{bmatrix} \begin{bmatrix} x_1(t;b) \\ x_2(t;b) \\ x_3(t;b) \\ x_4(t;b) \\ x_5(t;b) \end{bmatrix} = Cx(t;b) \tag{33}$$

thus leading to the following *two-stage* optimization:

$$\text{(Optimization II)}\begin{cases}\underset{b\in[b_1,b_2]}{\text{minimize}}\ \|y(t;b)-T_{\text{out}}\|^2_{L_2(0,\Delta t)}\\ \text{subject to}\\ \dot{x}(t;b)=\begin{cases}A_{\text{on}}(b)x(t;b)+B_{\text{in}}T_{\text{in}}(t)+B_{\text{out}}T_{\text{out}}(t), & t\in[0,t_s]\\ A_{\text{off}}(b)x(t;b)+B_{\text{in}}T_{\text{in}}(t)+B_{\text{out}}T_{\text{out}}(t), & t\in[t_s,\Delta t]\end{cases}\\ y(t;b)=Cx(t;b)\end{cases}\tag{34}$$

Therefore the optimal damping parameter can be written as

$$b^{opt}=\arg\min_{b\in(b_1,b_2)}\min_{t\in(0,\Delta t)}\left(\int_0^t(y_{\text{on}}(t;b)-T_{\text{out}})^2dt+\int_t^{\Delta t}(y_{\text{off}}(t;b)-T_{\text{out}})^2dt\right)\tag{35}$$

which essentially finds the optimal switch time $t_s$ for each value of the damping coefficient $b\in[b_1,b_2]$.

## 5 Numerical Results

Figure 6 depicts a sample run for different durations of the on-state expressed as percentages of the first duty cycle, ranging from 0.2% to 0.7%. The associated values of the error norm are tabulated in Table 2 for the same range of time durations. It is evident that an optimization of the switch time is warranted in order to provide the minimum deviation of the output $y(t)$ from $T_{\text{out}}$. It should be noted that even when the switching occurs at the instant the output is exactly equal to the output torque, this does not necessarily imply that it will stay at this value (i.e., stay at its equilibrium), since the time derivative of $\theta_3$ is not necessarily equal to zero at the instance of switching.

Combining the two levels of optimization for the optimal switch time that minimizes the $L_2$ norm of the error and the optimal damping coefficient (equivalently the damping ratio $\zeta$), we considered Optimization II in which seven values of the damping parameter representing damping rations in the range 0.02–0.12 were used to find the optimal switch times. Figure 7 depicts the error norm for various values of the damping ratio as a function of the percentage of a duty cycle in the on-state. Table 3 tabulates these results and provides an insight on the effects of damping ratio on switching times and on the error norm.

## 6 Discussion and Conclusion

Analyzing the dynamic system equations describing the switch-mode CVT in state-space form revealed some important points. First, a stable equilibrium does exist where the output torque stays at the desired output torque for the condition where the output shaft has zero velocity, namely, $\dot{\theta}_3=0$. Second, if $\dot{\theta}_3\neq 0$, the sys-

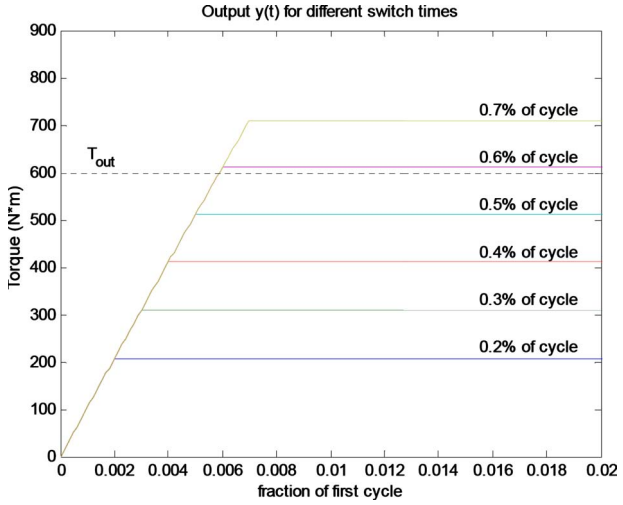


**Fig. 6 Evolution of the output $y(t)$ for different switch times. Switch times are expressed as a percentage of the first duty cycle, in the range 0.2–0.7%.**

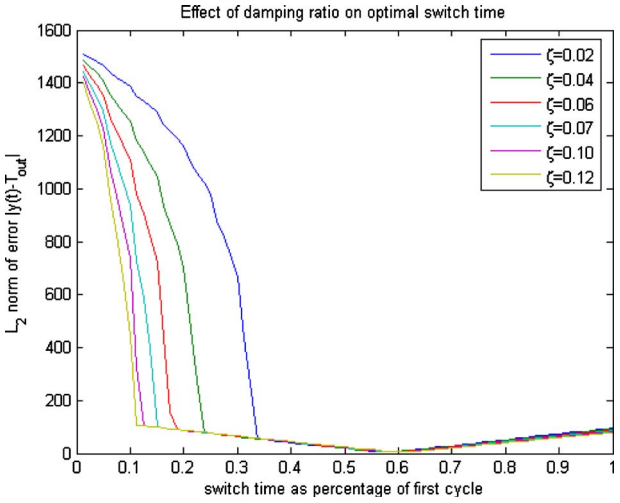


**Fig. 7 Effect of damping ratio on optimal switch time and optimal error norm. Switch time is expressed as a percentage of the first duty cycle.**

**Table 2 Different switch times expressed as percentages of the first duty cycle and the associated error norms**

| Percentage of duty cycle in the on-state (%) | Error norm |
|---|---|
| 0.2 | 88.0127 |
| 0.3 | 65.4133 |
| 0.4 | 43.0896 |
| 0.5 | 21.2616 |
| 0.6 | 6.1507 |
| 0.7 | 24.2381 |

**Table 3 Effect of damping on optimal switch time and optimal error norm**

| $\zeta$ | $t_s$ (% of duty cycle) | $L_2$ norm of error |
|---|---|---|
| 0.02 | 0.5750 | 5.8850 |
| 0.04 | 0.5875 | 5.9614 |
| 0.06 | 0.5875 | 5.9536 |
| 0.08 | 0.6000 | 5.9609 |
| 0.10 | 0.6000 | 6.0990 |
| 0.12 | 0.6125 | 6.2420 |

tem will never *reach and stay* at the desired torque due to the required switching between the two states of the system. Third, the largest $L_2$ norm error between the output torque and the desired torque occurs during the first duty cycle. For this reason, the analysis focused on the first switching period of the cycle.

The optimization of the first switching period was conducted in two stages. In the first stage, an optimal switch time from the on-state to the off-state was found that minimized the $L_2$ norm error for the first duty cycle. Because the system does not reach and stay at a desired output, the output torque trajectory must overshoot the desired torque to minimize the total error. For the specific desired torque output, the optimal switch time was found to be at approximately 0.6% duty cycle. In the second stage of the optimization, the influence of the spring damping on the error norm was investigated. It was discovered that the optimal switch time varied with the damping ratio, with the lowest error norm occurring at the lower range of damping ratios, which resulted in a lower optimal switch time.

The switch-mode CVT concept presented in this paper provides a novel solution to the challenge of efficiently and effectively coupling a high-speed flywheel to the drive train of a vehicle to create a flywheel hybrid system. The development of the dynamic system of equations, representation in state-space form, stability analysis, and optimization work build a foundation for future work. Specific areas of future work include analyzing and optimizing the system across multiple switching cycles and for tracking desired torque trajectories. The latter introduces several stability and optimization challenges: When switching over multiple cycles, one must ensure that stability under switching is preserved and that would impose a minimum of the switching instance above the dwell time [15]. Additionally, the switching instance might be different for each cycle and the torque trajectories might be time-varying. Furthermore, oversimplifying assumptions made in generating the system of equations will be relaxed to better represent the physical system.

## References


[1] 2008, "Department of Energy, Annual Energy Review 2008," Energy Information Administration (EIA), Report No. DOE/EIA-0384.

[2] Van de Ven, J. D., Olson, M. O., and Li, P. Y., 2008, "Development of a Hydro-Mechanical Hydraulic Hybrid Drive Train With Independent Wheel Torque Control for an Urban Passenger Vehicle," International Fluid Power Exposition, Las Vegas, NV, pp. 1–11.

[3] Eberhardt, J. J., 2002, "Fuels of the Future for Cars and Trucks," Diesel Engine Emissions Reduction (DEER), Workshop, San Diego, CA.

[4] Krivts, I. L., and Krejnin, G. V., 2006, *Pneumatic Actuating Systems for Automatic Equipment: Structure and Design*, CRC/Taylor & Francis, Boca Raton, FL.

[5] Bitterly, J. G., 1998, "Flywheel Technology: Past, Present, and 21st Century Projections," IEEE Aerosp. Electron. Syst. Mag., **13**(8), pp. 13–16.

[6] Genta, G., 1985, *Kinetic Energy Storage: Theory and Practice of Advanced Flywheel Systems*, Butterworths, London.

[7] Beachley, N. H., and Frank, A. A., 1979, "Flywheel Energy Management Systems for Improving the Fuel Economy of Motor Vehicles," University of Wisconsin, Report No. DOT/RSPA/DPB-50/79/1.

[8] Serrarens, A. F. A., Shen, S., and Veldpaus, F. E., 2003, "Control of a Flywheel Assisted Driveline With Continuously Variable Transmission," ASME J. Dyn. Syst., Meas., Control, **125**, pp. 455–461.

[9] Yimin, G., Gae, S. E., and Ehsani, M., 2003, "Flywheel Electric Motor/Generator Characterization for Hybrid Vehicles," IEEE Vehicular Technology Conference, Vol. 58, pp. 3321–3325.

[10] Brockbank, C., and Cross, D., 2009, "Mechanical Hybrid System Comprising a Flywheel and CVT for Motorsport & Mainstream Automotive Applications," SAE World Congress and Exposition, SAE, Detroit, MI, Vol. 2.

[11] Mohan, N., Robbins, W. P., and Undeland, T. M., 2003, *Power Electronics: Converters, Applications and Design*, Wiley, New York.

[12] Gilbert, J. M., Oldaker, R. S., Grindley, J. E., and Taylor, P. M., 1996, "Control of a Novel Switched Mode Variable Ratio Drive," *UKACC International Conference on Control*, University of Exeter, Exeter, UK, Vol. 1, pp. 412–417.

[13] Norton, R., 2001, *Cam Design and Manufacturing Handbook*, Industrial Press Inc., New York.

[14] Khalil, H. K., 2001, *Nonlinear Systems*, Prentice-Hall, New York.

[15] Liberzon, D., 2003, *Switching in Systems and Control*, Birkhäuser, Boston, MA.